ACS Infectious Diseases

pubs.acs.org/journal/aidcbc

Letter

Cariogenic *Streptococcus mutans* Produces Tetramic Acid Strain-Specific Antibiotics That Impair Commensal Colonization

Xiaoyu Tang,[#] Yuta Kudo,[#] Jonathon L. Baker,[#] Sandra LaBonte, Peter A. Jordan, Shaun M. K. McKinnie, Jian Guo, Tao Huan, Bradley S. Moore,* and Anna Edlund*

Cite This: *ACS Infect. Dis.* 2020, 6, 563−571

Read Online

ACCESS | Metrics & More | Article Recommendations | Supporting Information

ABSTRACT: *Streptococcus mutans* is a common constituent of dental plaque and a major etiologic agent of dental caries (tooth decay). In this study, we elucidated the biosynthetic pathway encoded by *muc*, a hybrid polyketide synthase and nonribosomal peptide synthetase (PKS/NRPS) biosynthetic gene cluster (BGC), present in a number of globally distributed *S. mutans* strains. The natural products synthesized by *muc* included three *N*-acyl tetramic acid compounds (reutericyclin and two novel analogues) and an unacylated tetramic acid (mutanocyclin). Furthermore, the enzyme encoded by *mucF* was identified as a novel class of membrane-associated aminoacylases and was responsible for the deacylation of reutericyclin to mutanocyclin. A large number of hypothetical proteins across a broad diversity of bacteria were homologous to MucF, suggesting that this may represent a large family of unexplored acylases. Finally, *S. mutans* utilized the reutericyclin produced by *muc* to impair the growth of neighboring oral commensal bacteria. Since *S. mutans* must be able to out-compete these health-associated organisms to persist in the oral microbiota and cause disease, the competitive advantage conferred by *muc* suggests that this BGC is likely to be involved in *S. mutans* ecology and therefore dental plaque dysbiosis and the resulting caries pathogenesis.

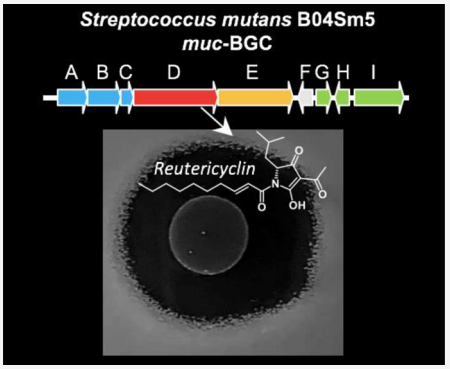

KEYWORDS: *oral microbiome, small molecule, biosynthesis, reutericyclin, antibacterial bioactivity*

The oral cavity harbors significant microbial diversity with over 700 constituent bacterial species described, which mainly colonize four physically distinct niches including dental plaque, tongue dorsum, buccal mucosa, and saliva.[1] Residents of dental plaque have been implicated in a variety of diseases, including dental caries, which affects more than a third of the world's population and results in approximately $300 billion in direct treatment costs to the global economy annually.[2−4] Although caries is a polymicrobial disease caused by a dysbiosis in the dental plaque microbial community, *Streptococcus mutans* is considered a primary etiologic agent. *S. mutans* is particularly adept at causing caries due to its exceptional capacity to form biofilms and its ability to survive acidic conditions that arrest acid production and growth in many more benign members of the oral microbiota.[5,6] To persist in the dental plaque community and cause disease, *S. mutans* must also be able to outcompete commensal bacteria directly.

Small molecules produced by biosynthetic gene clusters (BGCs) are increasingly recognized to play major roles in species−species communication and interactions.[7,8] Many *S. mutans* strains encode several types of BGCs, which include a group of bacteriocins, called mutacins, that contribute to *S. mutans* colonization and establishment in dental plaque.[9] Additionally, the mutanobactins, which are products of hybrid polyketide synthase and nonribosomal peptide synthetase (PKS/NRPS) origin, inhibit the morphological transition of *Candida albicans*.[10] A recent study further predicted 355 strain-specific BGCs across 169 *S. mutans* genomes,[11] suggesting that other genetically encoded small molecules in *S. mutans* may contribute to its biology. Previous bioinformatics efforts identified an orphan hybrid PKS/NRPS BGC (recently designated *muc*)[11,12] that is distributed among a subset of *S. mutans* strains. Within *muc*, five biosynthetic proteins are highly homologous (48%−69%) to cognates involved in the biosynthesis of reutericyclin (RTC) (Figures S1 and 1a).[13] RTC, which was discovered from sourdough isolates of *Lactobacillus reuteri*, acts as a proton ionophore antibiotic that modulates the microbial community of sourdough.[14,15] Interestingly, we found that *S. mutans* strains encoding *muc* were dispersed geographically and frequently associated with severe dental caries (Table S1). The goal of this study was to determine whether *muc* produces RTC or RTC-like molecules and if these molecules can affect the ability of *S. mutans* to compete with its neighbors.

Special Issue: Chemical Microbiology

Received: September 23, 2019
Published: January 6, 2020

https://dx.doi.org/10.1021/acsinfecdis.9b00365
ACS Infect. Dis. 2020, 6, 563−571

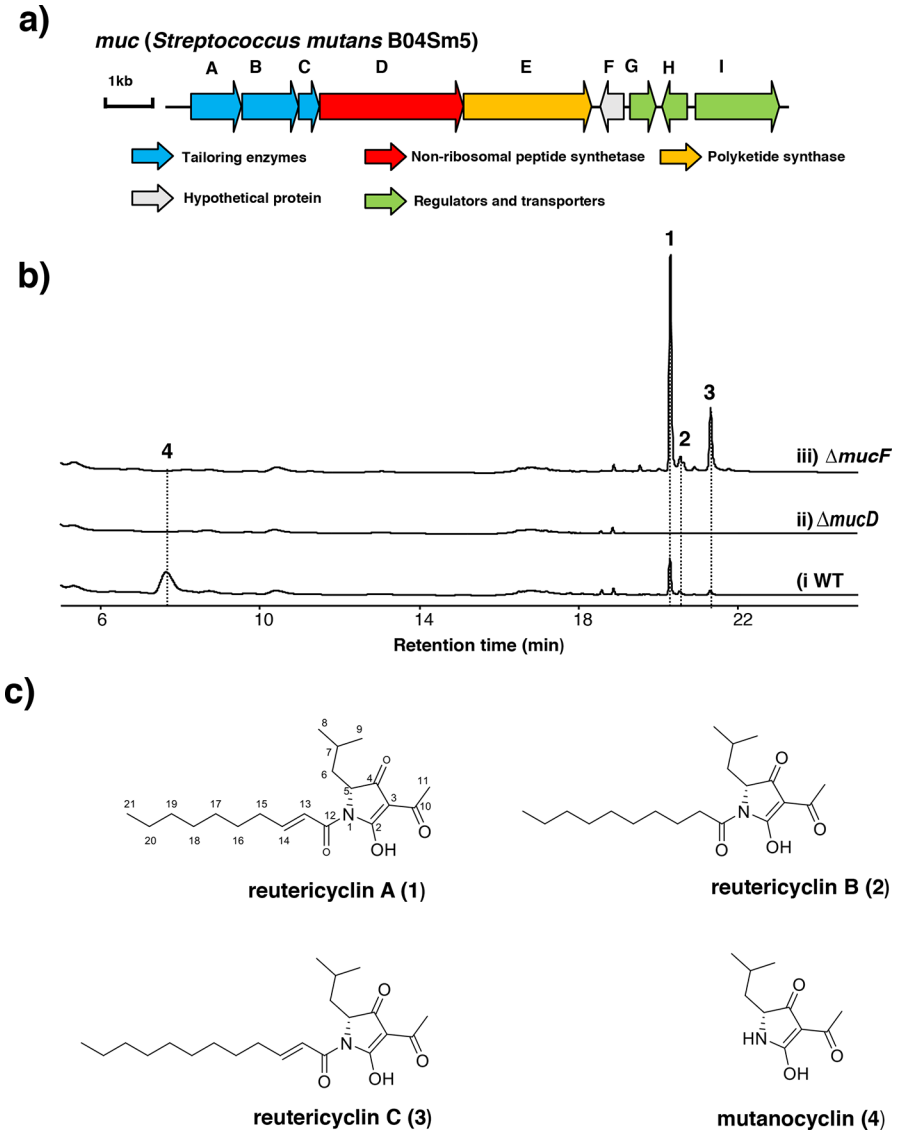

Figure 1. Identification of an orphan gene cluster from *S. mutans* and its metabolites. (a) Mutanocyclin gene cluster (*muc*) annotation. (b) HPLC profile of extracts from wild-type (WT) *S. mutans* B04Sm5 (i), *S. mutans* B04Sm5/Δ*mucD* (ii), and *S. mutans* B04Sm5/Δ*mucF* (iii). (c) Structures of metabolites identified from *S. mutans* in this study, including reutericyclin A (**1**), reutericyclin B (**2**), reutericyclin C (**3**), and mutanocyclin (**4**).

B04Sm5 *muc* is an ∼13 kb hybrid NRPS-PKS pathway encoding nine proteins (Figure 1a and Table S5). *In silico* analysis revealed that *mucD* and *mucE* encode the core assembly line protein machinery (Figures 1a and 2a). MucD is a C (condensation)−A (adenylation)−T (thiolation) tridomain protein, with specificity for adenylating leucine. MucE contains a KS (ketosynthase)-T-TE (thioesterase) module, commonly present in the termination modules of PKS assembly lines (Scheme 1). To determine the product(s) of *muc*, we utilized homologous recombination to delete the gene *mucD*, which encodes the predicted assembly line NRPS tridomain protein (Figure 1a). We conducted all our biosynthetic experiments in *S. mutans* B04Sm5, a strain bearing *muc*, which was isolated from a child with severe early childhood caries.[16] The B04Sm5 and Δ*mucD* mutant were cultured and extracted for HPLC analyses. The results showed that B04Sm5 produced four metabolites not present in the Δ*mucD* mutant (Figure 1b). These molecules were purified via preparative HPLC and characterized by high-resolution mass spectrometry (HR-MS/MS) and NMR experiments to reveal a group of tetramic acids, including RTC (renamed RTC A, **1**), two new RTC analogues (RTC B (**2**) and RTC C (**3**)), and a tetramic acid (**4**) (Figure 1c, Tables S2−S3, and Figures S2−S22). The structures of **1** and **4** were confirmed by chemical synthesis using a published method (Figures S8 and S15).[17,18] All the proton and carbon signals of new analogue **3** were assigned on the basis of the 2D NMR experiments. To determine the absolute configuration of **4**, chiral HPLC analysis was performed with the synthetic standards. Isolated **4** was observed as the mixture of *R*/*S* isomers in an 8:1 ratio (Figure S16). During preparation of this manuscript, Chen and colleagues published the identification of **4** (designated mutanocyclin (MUC) using a new heterologous expression system.[12] However, the production of **1**−**3** in both heterologous host and wild-type producers was not reported. The absolute configuration of **1** was analyzed by chiral HPLC with a synthetic standard and isolated (*R*)-**1** from *L. reuteri* LTH2584,[14] revealing the (*R*)-configuration at C-5 in isolated **1** from *S. mutans* (Figure S9).

https://dx.doi.org/10.1021/acsinfecdis.9b00365
ACS Infect. Dis. 2020, 6, 563−571

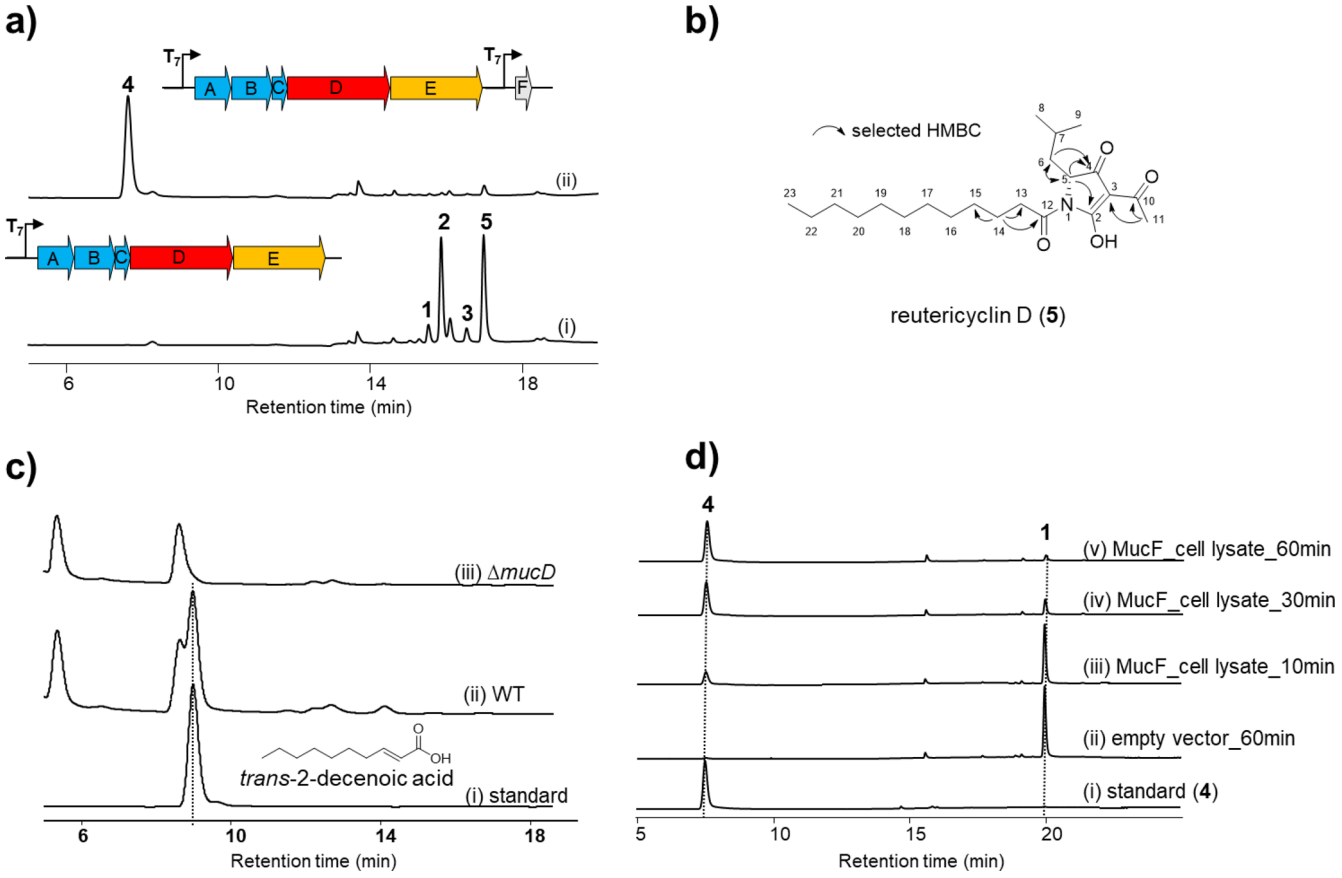

Figure 2. Characterization of MucF as acylase. (a) HPLC profiles of extracts from *E. coli* BAP1/pEXT06 (*mucA*−*D*) (i) and *E. coli* BAP1/pEXT07 (*mucA*−*D* + *mucF*) (ii). (b) Key HMBC correlations of compound **5**. (c) HPLC analysis of *trans*-2-decenoic acid standard (i) extracts from wild-type (WT) *S. mutans* B04Sm5 (ii) and *S. mutans* B04Sm5/Δ*mucD* (iii). (d) HPLC analysis of isolated **4** as a standard (i), compound **1** incubated with *E. coli* Rosetta2 (DE3)pLys/pET28a (empty vector) cell lysate for 60 min (ii), and compound **1** incubated with *E. coli* Rosetta2 (DE3)pLys/pEXT26 (carrying *mucF*) for 10 min (iii), 30 min (iv), and 60 min (v).

Scheme 1. Model for 1−4 Biosynthesis[a]

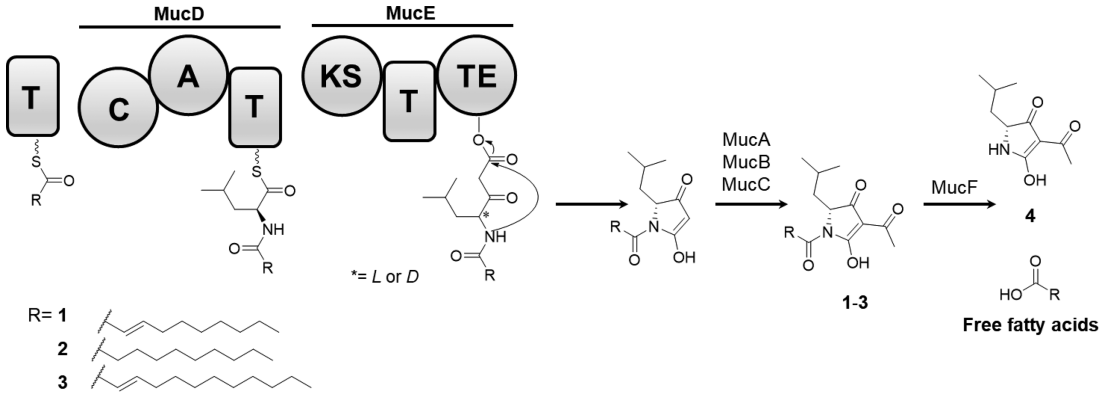

[a]C, condensation; A, adenylation; T, thiolation; KS, ketosynthase; TE, thioesterase.

On the basis of the enzymatic logic of thiotemplate-mediated assembly line biosynthesis, we propose that **1**−**3** are assembled, respectively, from *trans*-2-decenoyl-ACP (acyl carrier protein), decanoyl-ACP, and *trans*-2-dodecenoyl-ACP starter units through elongation with leucine, followed by elongation with a malonyl-CoA extender unit (Scheme 1). The inspection of structures of **1**−**3** suggested that the A domain of MucD appears to install a D-leucine residue into the final product. To explore this hypothesis, we fed both [$^{13}C_1$] L- and D-leucine to cultures of *S. mutans* B04Sm5. MS analyses of the purified **1** and **3** only revealed the incorporation of [$^{13}C_1$] L-leucine (Figures S23 and S24). The same result was observed by feeding the original RTC producer *L. reuteri* with the same isomers (Figure S25). These results indicate that an unrecognized epimerization reaction is involved in **1**−**3** biosynthesis; however, no standard epimerization (E) domain or dual functioning C/E domains could be found either in the assembly line or encoded elsewhere in the BGC. Additionally,

https://dx.doi.org/10.1021/acsinfecdis.9b00365
ACS Infect. Dis. 2020, 6, 563−571

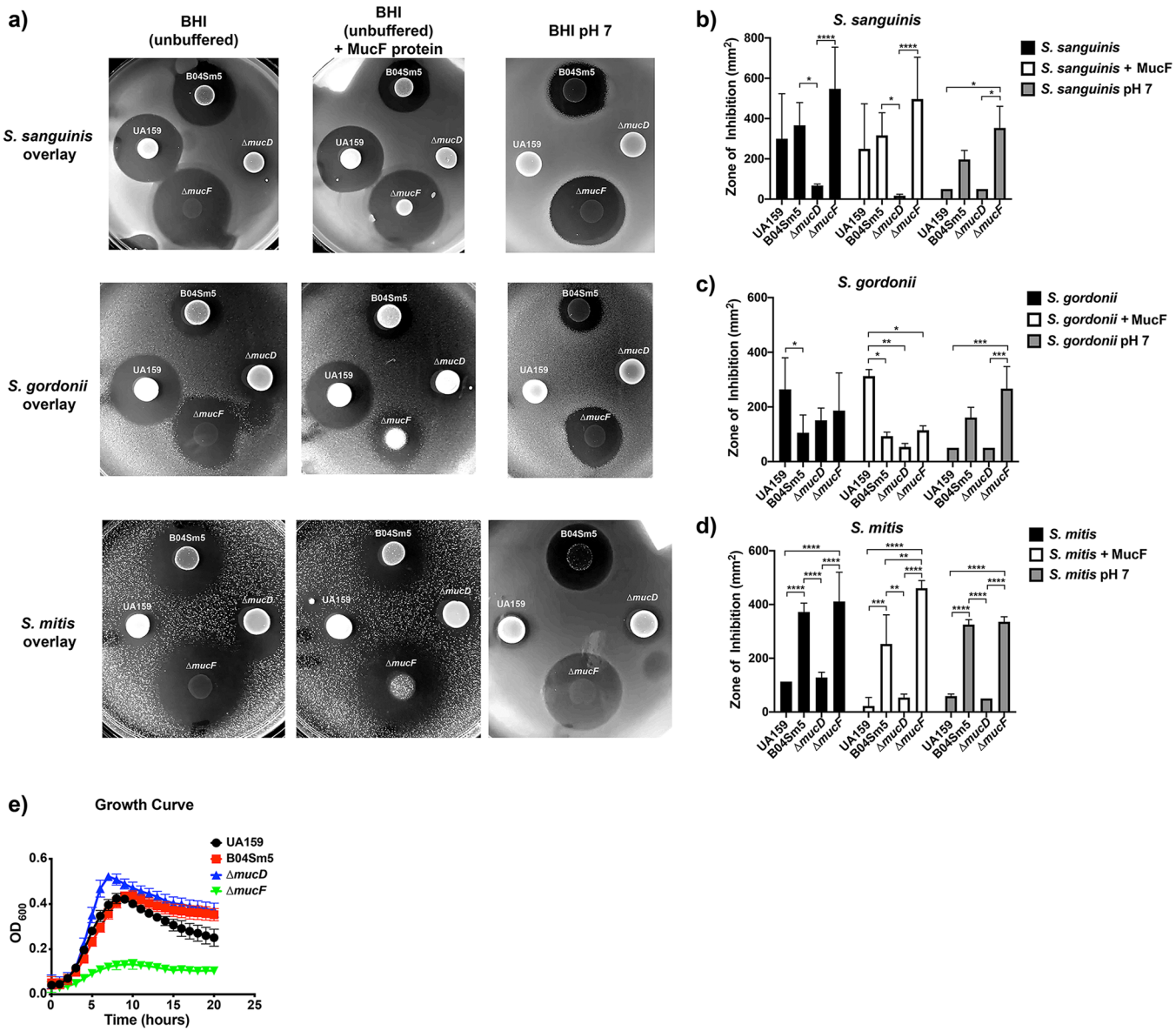

Figure 3. *S. mutans* uses the chemicals synthesized by *muc* to inhibit the growth of the competing species. (a) Deferred-antagonism assay, performed as described in the Methods, to observe the inhibition of other species by *S. mutans*. Cultures of *S. mutans* UA159, B04Sm5, Δ*mucD*, and Δ*mucF* were spotted on BHI agar or BHI agar buffered to pH 7 and incubated overnight. Cultures of *S. sanguinis*, *S. gordonii*, or *S. mitis* were added to 5 mL of soft BHI agar or pH 7 BHI agar and used to overlay the plates containing the *S. mutans* strains. Where indicated, 8 μL of purified MucF acylase protein was added to the spot of *S. mutans* and incubated for 3 h prior to the overlay with the 2nd species. Zones of inhibition were measured 24 h after addition of the assay. (b–d) Bar graphs illustrating the zones of inhibition produced by the indicated strains and conditions. Error bars represent standard deviation, and asterisks denote the statistical significance between indicated pairs as determined by Tukey's multiple-comparison test following a two-way ANOVA (*, $P < 0.05$; **, $P < 0.01$; ***, $P < 0.001$; ****, $P < 0.0001$) ($n = 4$). (e) Growth kinetics of the Δ*mucF* strain is impaired. Graph illustrating the growth of UA159, B04Sm5, Δ*mucD*, and Δ*mucF* in BHI ($n = 8$).

although a dual-function TE/E domain has been characterized from the nocardicin (NOC) biosynthetic assembly line,[19] MucTE shows very low homology (20%/35%, identity/similarity) to the dual functioning NocTE domain.

The first three genes (*mucA*–*C*) encode a hydroxymethylglutaryl-CoA synthase (MucA), a thiolase (MucB), and a hypothetical protein (MucC) (Table S5), which show homology to the three subunits (PhlA, PhlB, and PhlC, respectively) of a multicomponent C-acetyltransferase involved in the acetylation of the type III PKS product phloroglucinol from *Pseudomonas fluorescens* Q2-87.[20,21] As the combination of the three genes was also identified in *rtc* (*rtcA*, *rtcC*, and *rtcB*) from *L. reuteri*,[13] the function of MucA–C is consistent with introducing the acetyl group to the pyrrolidine ring of **1**–**3** (Scheme 1). We additionally annotated four genes downstream of the *mucA*–*E* operon encoding a small HXXEE domain-containing membrane-protein (MucF) of unknown function, two TetR/AcrR family transcriptional regulators (MucG and MucH), and one multidrug efflux pump (MucI) (Table S5). Presumably, *mucFGHI* is not involved in the direct synthesis of **1**–**3**. To verify this hypothesis, we cloned the operon from *mucA* to *mucE* into the pACYCDuet-1 vector to generate the plasmid pEXT06, in which the operon is exclusively under control of a T_7 promoter. As expected, the expression of the *mucA*–*E* in *Escherichia coli* BAP1 strain resulted in the production of at

https://dx.doi.org/10.1021/acsinfecdis.9b00365
ACS Infect. Dis. 2020, 6, 563–571

least four products, including **1**−**3** and new compound **5** (Figures 2a,b and S26). Compound **5** was purified via preparative HPLC, and its structure was further confirmed as a new RTC analogue (RTC D) possessing a *N*-dodecanoyl substituent by MS and detailed NMR analyses (Figure 2b, Table S4, and Figures S26−S30). This result indicates that the first six genes *mucA*−*E* indeed compose the minimal BGC for **1**−**3** production (Scheme 1). It seems likely that the different ratios of compounds **1**−**3** and the presence of compound **5** observed in *E. coli* are due to distinct concentrations of the various fatty acid precursors available for biosynthesis in *E. coli* versus *S. mutans*.

As the structure of **4** is consistent with the RTC core lacking the fatty acyl chain, we examined whether the free fatty acid, *trans*-2-decenoic acid, per compound **1**, is present in the extract of *S. mutans* B04Sm5. HPLC analyses confirmed that *S. mutans* B04Sm5 readily produced *trans*-2-decenoic acid (Figure 2c). In contrast, it was not detected in the pathway-deficient mutant *S. mutans* B04Sm5/Δ*mucD* (Figure 2c). These findings suggested that **4** may be derived from **1**−**3** via deacylation by an unknown mechanism. Interestingly, *trans*-2-decenoic acid is a known *Streptococcus* diffusible signal factor (SDSF) isolated from many *Streptococcus* species,[22] which inhibits the hyphal formation of the opportunistic fungus *Candida albicans*. Among the annotated pathway enzymes, only the function of MucF was unassigned. The MucF protein sequence was subjected to a secondary structure prediction-based homology search (Phyre2), which suggested it is a polytopic (five) transmembrane α-helical protein (Figure S31) with low similarity (15%) to a viral protein (PDB 3LD1) with putative hydrolase activity. To explore whether MucF might be involved in the deacylation of **1**−**3**, we generated a *mucF* deletion mutant in *S. mutans* B04Sm5. HPLC analysis of the extract of mutant cultures illustrated that the Δ*mucF* mutant not only increased the production of **1**−**3** by ∼3−5-fold but also lost the ability to produce **4** (Figure 1b). These findings strongly suggested that MucF is essential for converting **1**−**3** to **4**. To further evaluate the function of MucF, we cloned and expressed *mucF* in *E. coli* and incubated **1** with the *E. coli*/*mucF* cell lysate, leading to the *in vitro* production of the deacylated **4** (Figure 2d). In contrast, no conversion was detected in the control experiment (*E. coli* carrying empty vector) (Figure 2d). To further support this observation, we inserted a copy of *mucF* into the secondary expression site of pEXT06, resulting in the plasmid pEXT07. Its expression in *E. coli* BAP1 further led to the formation of **4** (Figure 2a). Collectively, these results strongly support that MucF is a newly recognized deacylase responsible for converting **1**−**3** to **4**. Notably, MucF showed sequence similarity to a large group of hypothetical proteins from the genomes of bacteria associated with the human gut and skin (Figure S32). We therefore speculate MucF joins a large family of unrecognized aminoacylases that may play important roles within the human microbiota.

While the antimicrobial activity of reutericyclin A (**1**) has been well-documented against a number of taxa, synthesized mutanocyclin (**4**) did not show significant antimicrobial activity.[23] Since *S. mutans* must be able to outcompete its neighbors in the oral microbiome to persist and cause disease, we examined whether *S. mutans* utilized *muc* and **1**−**4** in mediating interspecies interactions. A simple colony-versus-colony inhibition screen indicated that *S. mutans* UA159 (the type strain for *S. mutans* and a model organism for caries disease), B04Sm5, Δ*mucD*, and Δ*mucF* were capable of inhibiting the growth of adjacent colonies of *Rothia mucilaginosa*, *Streptococcus sanguinis*, *Streptococcus gordonii*, *Streptococcus mitis*, *Streptococcus pneumoniae*, and *Streptococcus salivarius* to varying degrees (Figure S33). Δ*mucF* exhibited the greatest inhibition of the other taxa, followed by B04Sm5, UA159, and then Δ*mucD* (Figure S33). The antagonistic relationships between *S. mutans* and its competitors, *S. sanguinis*, *S. gordonii*, and *S. mitis* are well-characterized and play an important role in caries development; therefore, the interaction between *muc* and these species was explored in more depth (Figure 3).[24,25] B04Sm5 and Δ*mucF* produced sizable zones of inhibition in agar overlays of *S. sanguinis*, *S. gordonii*, and *S. mitis*, while UA159 produced a large zone of inhibition in overlays of *S. sanguinis* and *S. gordonii* but a small zone of inhibition in *S. mitis* (Figure 3A−D). Δ*mucD* consistently produced greatly reduced zones of inhibition, while Δ*mucF* consistently produced larger zones of inhibition than B04Sm5. The addition of purified MucF enzyme on top of the initial colonies, followed by 3 h of incubation prior to the addition of the agar overlay, allowed the growth of a colony of the second species in the previously inhibited zone. This was quite noticeable over the Δ*mucF* colonies, as the growth of the original Δ*mucF* colony was not very robust (Figure 3A, middle column of panels). Collectively, this data supports the hypotheses that *S. mutans* utilizes the chemicals produced by *muc* to inhibit neighboring species and that the acylated natural products (**1**−**3**) are much more antimicrobial than **4** (Figure 3). Because *S. mutans* is a well-known acid producer, the growth inhibition assay was also conducted in media buffered to pH 7 to determine to what extent the acids produced by fermentation played in inhibiting the competing species (Figure 3). On buffered media, inhibition by UA159 was greatly reduced, while B04Sm5 and Δ*mucF* still significantly inhibited the competing species, indicating that the chemical(s) produced by *muc*, and not acidic fermentation end-products, were the significant sources of the zones of inhibition produced by these strains. BGC mining results, obtained by using the antiSMASH software, revealed that the B04Sm5 genome encodes five putative mutacins, which all have homologues in the UA159 genome. In addition, the B04Sm5 genome harbors one putative lantibiotic BGC and the *muc* BGC. Lantibiotics are known for their antimicrobial activities, but since the activity in the Δ*mucD* strain was greatly reduced, it is clear that the observed inhibition is due to the production of **1**−**3**. Reutericyclin is already well-known for its high antimicrobial activity.[15] None of the *S. mutans* strains significantly inhibited the growth of each other under the conditions tested (data not shown). Growth curves indicated that UA159, B04Sm5, and Δ*mucD* all had similar growth kinetics, while the growth of Δ*mucF* was significantly impaired, providing further evidence that the MucF acylase serves has an "antitoxin" to RTC in *S. mutans* (Figure 3E). Taken together, these results indicate that *S. mutans* strains containing *muc* modulate the growth of their bacterial neighbors using the small molecules assembled by this BGC. The increased competitive fitness conferred by *muc* is likely to increase the virulence of *S. mutans* strains bearing this gene cluster. As *S. mutans* is an exceptionally productive biofilm-former, higher numbers of *S. mutans* are likely to increase plaque biofilm formation and promote the dysbiosis, which leads to the formation of caries lesions.[5,6] Additional studies examining the role of *muc* in more complex and clinically relevant ecological settings are currently in progress. Interestingly, Chen and

https://dx.doi.org/10.1021/acsinfecdis.9b00365
ACS Infect. Dis. 2020, 6, 563−571

colleagues showed that **4** can significantly suppress the infiltration of leukocytes ($CD45^+$ cells) into the Matrigel plug in a mouse model, suggesting an anti-inflammatory activity.[12]

In summary, we describe a versatile biosynthetic pathway from an oral pathogen, *S. mutans* B04Sm5, which can produce three types of compounds with divergent biological activities. These include three *N*-acyl tetramic acids (**1**−**3**) that display antibacterial properties against oral commensal bacteria, a new tetramic acid (**4**) with a reported anti-inflammatory activity in a mouse model,[12] and a previously characterized SDSF with the ability to interact with pathogenic oral fungi.[22] While this study merely scrapes the "tip of the iceberg" of the recently identified biosynthetic potential of the oral microbiota,[7,26] these findings exemplify that deeper exploration of leads provided by chemical and genome mining studies will help elucidate the complex ecological underpinnings of the human microbiome and its relationship to disease.

METHODS

General Methods. A complete list of the primers, plasmids, and strains used in this study can be found in Table S6. PCR products were amplified with PrimeSTAR HS DNA polymerase (Clontech Laboratories, Inc., USA). DNA isolations and manipulations were carried out using standard protocols. *Escherichia coli* strains were cultivated in LB medium (Thermo Fisher Scientific, USA) supplemented with appropriate antibiotics. *S. mutans* B04Sm5 and its respective derivatives were all grown on Brain Heart Infusion (BHI) agar or liquid medium (BD Biosciences, USA) at 37 °C in a CO_2 incubator (5% CO_2/95% air). *Lactobacillus reuteri* LTH2584 was grown on MRS medium (BD Biosciences, USA) or agar at 37 °C in a CO_2 incubator (5% CO_2).

Construction of *S. mutans* Knockout Plasmids. A 1010-bp fragment containing the spectinomycin resistance gene ($spec^R$) was amplified from pCAPB2[27] with primers spec_fwd and spec_rev (Table S6). The left (532 bp) and right (555 bp) flanking regions of *mucD* were amplified from the genomic DNA of *S. mutans* B04Sm5 with the primer pairs of mucD_KO_L-fwd/mucD_KO_L-rev and mucD_KO_R-fwd/mucD_KO_R-rev (Table S6), respectively. These three PCR products were assembled with a double digested pUC19 (*Pst*I and *Eco*RI) using a NEBuilder HiFi DNA Assembly kit (New England Biolabs, USA), which resulted in the vector pEXT01. Amplification of the left (602 bp) and right (611 bp) flanking regions of *mucF* was accomplished with primer pairs mucF_KO_L-fwd/mucF_KO_L-rev and mucF_KO_R-fwd/mucF_KO_R-rev (Table S6), respectively. These two PCR products and the $spec^R$ gene were cloned into pUC19 to give pEXT02 using the method described above. Vector clones were verified by restriction analysis and sequencing.

Generation of Δ*mucD* and Δ*mucF* Mutants. The disruption cassettes were amplified from pEXT01 (2159 bp) and pEXT02 (2159 bp) using primer pairs mucD_KO_L-fwd/mucD_KO_R-rev and mucF_KO_L-fwd/mucF_KO_R-rev (Table S6), respectively. PCR products were digested by DpnI and then purified using the QIAquick PCR Purification Kit (Qiagen, USA). The disruption cassettes were transformed to *S. mutans* B04Sm5 by a previously reported protocol.[28] Δ*mucD* and Δ*mucF* deletion mutants were selected by the growth on BHI agar supplemented with 500 μg/mL spectinomycin, confirmed by PCR and sequencing, and designated as *S. mutans* B04Sm5/Δ*mucD* and *S. mutans* B04Sm5/Δ*mucF*.

Generation of *muc* Expression Plasmid. The 8.6-kb DNA region containing *mucA*−*E* was PCR amplified from the genomic DNA of *S. mutans* B04Sm5 in two fragments (each approximately 4 kb) with primer pairs mucA-E_fwd1/mucA-E_rev1 and mucA-E_fwd2/mucA-E_rev2 (Table S6). These fragments were cloned into the XhoI site of pACYCDuet-1 by a NEBuilder HiFi DNA Assembly kit (New England Biolabs, USA), resulting in the plasmid pEXT06. To construct pEXT07, *mucF* was amplified with primers mucF-coexp_fwd and mucF_coexp_rev. The PCR product and pEXT06 were digested with the restriction enzyme pair NcoI/*Bam*HI and ligated with T4 DNA ligase (New England Biolabs, USA). The resulting vectors were verified by restriction analysis and sequencing. pEXT06 and pEXT07 were transformed into *E. coli* BAP1, respectively.

Expression, Extraction, and Detection of *muc* Expression in *E. coli* BAP1. *E. coli* BAP1 containing pEXT06 or pEXT07 was cultivated on LB plates supplemented with 1% glucose and 50 μg/mL chloramphenicol at 37 °C. The following day, a loop of *E. coli* cells was transferred for precultures grown at 37 °C in 10 mL of LB medium supplemented with 1% glucose and 50 μg/mL chloramphenicol for 4−5 h. One microliter of each preculture was transferred to 50 mL of fresh LB with the same supplements and grown at 37 °C to an OD_{600} of 0.4 to 0.6. Cultures were induced with 200 μM IPTG and incubated for an additional 12−14 h at 30 °C with shaking (220 rpm). Cultures were harvested, and 1 mL of H_2O supplemented with 0.5 mg/mL lysozyme was added to the pellets. Cells were disrupted by sonication at room temperature. The lysates were acidified with acetic acid (1% final concentration) and extracted twice with an equal volume of EtOAc. The organic phase was evaporated, resuspended in MeOH (0.2 mL), and filtered through Acrodisc MS PTFE Syringe filters (Pall Inc., Ann Arbor, MI, USA) prior to HPLC analysis. Each extract was monitored at 280 nm during separation by HPLC using a Kinetex C18 100 Å, LC Column (5 μm, 150 × 2.1 mm; Phenomenex, US) as follows: 0−10 min, 30% B; 10−11 min, 30%−100% B; 11−25 min, 100% B; 26−27 min, 100%−30% B; 28−35 min, 30% B (solvent A: H_2O/TFA (999:1, v/v); solvent B: CH_3CN/TFA (999:1)).

Expression and Activity Testing of MucF in *E. coli*. Primer pair mucF_pET_fwd/mucF_pET_rev (Table S6) was used for amplification of *mucF* from the genomic DNA of *S. mutans* B04Sm5. The PCR product was cloned into the NcoI and XhoI sites of pET28a to obtain pEXT26 (with a C-terminal His-tag). Next, pET28a and pEXT26 were transferred into *E. coli* Rosetta2 (DE3)pLys, respectively. Single clones were picked for precultures grown overnight at 37 °C in TB broth (Thermo Fisher Scientific, USA) with 50 μg/mL kanamycin and 50 μg/mL chloramphenicol at 37 °C. One microliter of preculture was transferred to 1 L of fresh TB broth with the same antibiotics and grown at 37 °C to an OD_{600} of 0.4 to 0.6. Cultures were induced with 500 μM IPTG and incubated for an additional 16 h at 18 °C with shaking (220 rpm). Cultures were harvested, and 10 mL of buffer (50 mM Tris-HCl, pH 8, 150 mM NaCl, 10% glycerol) supplemented with 0.5 mg/mL lysozyme and 0.5 mM PMSF was added to the pellets. Cells were disrupted by sonication at 4 °C. The lysate was used for MucF activity testing. The assay mixture for the reaction (100 μL) consisted of 96 μL of *E. coli*

https://dx.doi.org/10.1021/acsinfecdis.9b00365
ACS Infect. Dis. 2020, 6, 563−571

lysate (both carrying empty pET28a or pEXT26) and 4 μL of reutericyclin A (**1**) solution (6.6 mM, 80% EtOH). The reaction solutions were prepared on ice and incubated at 37 °C for 10, 30, and 60 min. Reactions were terminated by the addition of 1 μL of acetic acid and then extracted twice with 200 μL of EtOAc. After centrifugation of the assay at 12 000*g* for 10 min, the organic phase was evaporated and resuspended in 100 μL of MeOH (0.2 mL). The extracts were monitored by HPLC.

Deferred-Antagonism Assay. The deferred-antagonism assay was performed as previously described.[29] Briefly, 8 μL of overnight cultures of UA159, B04Sm5, Δ*mucD*, and Δ*mucF* was spotted onto BHI + 1% agar or BHI + 1% agar that was buffered to pH 7 with 1 M KH_2PO_4/K_2HPO_4, pH 7.5, and incubated overnight at 37 °C under 5%CO_2/95% air. The following day, the plates were sterilized using the sterilization setting (90 s) in a GS Gene Linkter UV chamber (Bio-Rad, Inc.). Where applicable, 8 μL of purified MucF protein was spotted onto the colonies of *S. mutans*, and it was incubated for 3 h at 37 °C. 500 μL of overnight cultures of *S. sanguinis*, *S. gordonii*, or *S. mitis* was added to 5 mL of molten BHI + 0.75% agar or BHI + 0.75% that was buffered to pH 7 with 1 M KH_2PO_4/K_2HPO_4, pH 7.5, that had been cooled to 40 °C, and this was used as an overlay over the plates with the *S. mutans* colonies. The agar overlay was allowed to solidify at RT, and then, plates were incubated overnight at 37 °C under 5% CO_2/95% air. Zones of inhibition were measured the following day.

Growth Curve. Ten microliters of overnight cultures of UA159, B04Sm5, Δ*mucD*, and Δ*mucF* was added to 200 μL of BHI in a 96-well plate. Growth was monitored using a Tecan Infinite Nano. Optical density at 600 nm (OD_{600}) was measured every hour for 24 h under 37 °C, with 5 s of shaking prior to each reading. Eight replicates of each strain were monitored.

Other Methods. Other methods, including BGC mining in *S. mutans* genomes, annotations of the *muc* BGC, isolation, synthesis, and structural elucidation of reutericyclins and mutanocyclin, and the identification of MucF orthologous groups, are described in the Supporting Information Methods.

■ ASSOCIATED CONTENT

Supporting Information

The Supporting Information is available free of charge at https://pubs.acs.org/doi/10.1021/acsinfecdis.9b00365.

Supplementary methods and materials; synthesis of mutanocyclin (**4**) and reutericyclin A (**1**); Table S1: sequenced strains with *muc* pathways distributed globally; Table S2: NMR spectroscopic data of compound **1**, reutericyclin A, in CDCl3; Table S3: NMR spectroscopic data of compound **3**, reutericyclin C ((*E*)-dodec-2-enoyl-reutericyclin), in CDCl3; Table S4: NMR spectroscopic data of compound **5**, reutericyclin D, in CDCl3; Table S5: deduced function of genes from the *muc* gene cluster in *Streptococcus mutans* B04Sm5; Table S6: plasmids, primers, and strains used in this study; Figure S1: comparison of *muc* and *rtc* gene clusters; Figure S2: high-resolution MS/MS spectrometry analysis of compounds **1**−**4** isolated from *S. mutans* B04Sm5; Figure S3: ^{1}H NMR spectrum of **1**; Figure S4: ^{13}C NMR spectrum of **1**; Figure S5: COSY spectrum of **1**; Figure S6: HSQC spectrum of **1**; Figure S7: HMBC spectrum of **1**; Figure S8: comparison of the isolated **1** with synthetic standards; Figure S9: comparison of compound **1** with synthetic and isolated standards by chiral HPLC; Figure S10: ^{1}H NMR spectrum of **3**; Figure S11: ^{13}C NMR spectrum of **3**; Figure S12: COSY spectrum of **3**; Figure S13: HSQC spectrum of **3**; Figure S14: HMBC spectrum of **3**; Figure S15: comparison of the isolated **4** with synthetic standards; Figure S16: comparison of **4** with synthetic standards by chiral HPLC; Figure S17: ^{1}H NMR spectrum of synthetic (*R*)-**4**; Figure S18: ^{13}C NMR spectrum of synthetic (*R*)-**4**; Figure S19: COSY spectrum of synthetic (*R*)-**4**; Figure S20: HSQC spectrum of synthetic (*R*)-**4**; Figure S21: HMBC spectrum of synthetic (*R*)-**4**; Figure S22: chiral HPLC analysis of synthetic (*S*)-**4** and (*R*)-**4**; Figure S23: MS analysis of **1** isolated from *S. mutans* B04Sm5 feeding experiments; Figure S24: MS analysis of **3** isolated from *S. mutans* B04Sm5 feeding experiments; Figure S25: MS analysis of **1** isolated from *L. reuteri* LTH25841 feeding experiments; Figure S26: high-resolution MS/MS spectrometry analysis of **1**−**5** isolated from an *E. coli* BAP1 expression host; Figure S27: ^{1}H NMR spectrum of **5**; Figure S28: COSY spectrum of **5**; Figure S30: HMBC spectrum of **5**; Figure S31: MucF is predicted as a putative membrane-bound protein; Figure S32: maximum likelihood (ML) tree of *S. mutans* B04Sm5MucF; Figure S33: interspecies competition assay (PDF)

■ AUTHOR INFORMATION

Corresponding Authors

Bradley S. Moore − *Scripps Institution of Oceanography, University of California San Diego, La Jolla, California 92093-0204, United States; Skaggs School of Pharmacy and Pharmaceutical Sciences, University of California at San Diego, La Jolla, California 92093, United States;* orcid.org/0000-0002-4652-1253; Email: bsmoore@ucsd.edu

Anna Edlund − *Genomic Medicine Group, J. Craig Venter Institute, La Jolla, California 92037, United States;* orcid.org/0000-0002-3394-4804; Email: aedlund@jcvi.org

Authors

Xiaoyu Tang − *Genomic Medicine Group, J. Craig Venter Institute, La Jolla, California 92037, United States; Scripps Institution of Oceanography, University of California San Diego, La Jolla, California 92093-0204, United States;* orcid.org/0000-0002-7855-5984

Yuta Kudo − *Scripps Institution of Oceanography, University of California San Diego, La Jolla, California 92093-0204, United States;* orcid.org/0000-0002-1586-2004

Jonathon L. Baker − *Genomic Medicine Group, J. Craig Venter Institute, La Jolla, California 92037, United States*

Sandra LaBonte − *Genomic Medicine Group, J. Craig Venter Institute, La Jolla, California 92037, United States; Department of Biochemistry and Biophysics, Texas A&M University and Texas AgriLife Research, College Station, Texas 77843-2128, United States*

Peter A. Jordan − *Scripps Institution of Oceanography, University of California San Diego, La Jolla, California 92093-0204, United States*

https://dx.doi.org/10.1021/acsinfecdis.9b00365
ACS Infect. Dis. 2020, 6, 563−571

Shaun M. K. McKinnie − *Scripps Institution of Oceanography, University of California San Diego, La Jolla, California 92093-0204, United States;* orcid.org/0000-0001-6776-6455
Jian Guo − *Department of Chemistry, University of British Columbia, Vancouver, British Columbia V6T 1Z1, Canada*
Tao Huan − *Department of Chemistry, University of British Columbia, Vancouver, British Columbia V6T 1Z1, Canada;* orcid.org/0000-0001-6295-2435

Complete contact information is available at: https://pubs.acs.org/10.1021/acsinfecdis.9b00365

Author Contributions

#X.T., Y.K., and J.L.B. contributed equally to this work. X.T., J.L.B., and A.E. designed the research, and X.T. analyzed the *muc* pathway. X.T. generated and analyzed the mutants and performed the biochemical experiments and the heterologous expression experiments. Y. K. and X.T. purified the compounds and elucidated the structures of all the compounds. X.T., P.A.J., and S.M.K.M. performed the chemical synthesis. X.T., Y.K., J.G., and T.H. performed mass spectrometry experiments and analyzed mass spectrometry data. X.T., J.L.B., and S.L. designed and performed the agar plate-based assays and growth curve. X.T., Y.K., J.L.B., A.E., and B.S.M. wrote the manuscript. All authors analyzed and discussed the data and contributed to the writing of the manuscript.

Notes

The authors declare no competing financial interest.

■ ACKNOWLEDGMENTS

The authors thank Y. Li (NYU College of Dentistry, USA) for providing the *S. mutans* strain B04Sm5, M.G. Gänzle (University of Alberta, Canada) for providing the *L. reuteri* LTH2584 strain, C. Khosla (Stanford University, USA) for *E. coli* BAP1, and J.J. Zhang (Massachusetts Institute of Technology, USA), M.S. Donia (Princeton University, USA), and M.A. Fischbach (Stanford University, USA) for valuable discussions. This work was supported by NIH grants R00-DE0245543 and R21-DE028609-01 (to A.E.), R01-GM085770 (to B.S.M.), and F32-DE026947 (to J.L.B.) and the Japan Society for Promotion of Science Overseas Research Fellowship (to Y.K.).

■ REFERENCES

(1) Aas, J. A., Paster, B. J., Stokes, L. N., Olsen, I., and Dewhirst, F. E. (2005) Defining the normal bacterial flora of the oral cavity. *J. Clin Microbiol 43* (11), 5721−32.
(2) Listl, S., Galloway, J., Mossey, P. A., and Marcenes, W. (2015) Global Economic Impact of Dental Diseases. *J. Dent. Res. 94* (10), 1355−61.
(3) Pitts, N. B., Zero, D. T., Marsh, P. D., Ekstrand, K., Weintraub, J. A., Ramos-Gomez, F., Tagami, J., Twetman, S., Tsakos, G., and Ismail, A. (2017) Dental caries. *Nat. Rev. Dis Primers 3*, 17030.
(4) GBD 2017 Disease and Injury Incidence and Prevalence Collaborators (2018) Global, regional, and national incidence, prevalence, and years lived with disability for 354 diseases and injuries for 195 countries and territories, 1990−2017: a systematic analysis for the Global Burden of Disease Study 2017. *Lancet 392* (10159), 1789−1858.
(5) Bowen, W. H., Burne, R. A., Wu, H., and Koo, H. (2018) Oral Biofilms: Pathogens, Matrix, and Polymicrobial Interactions in Microenvironments. *Trends Microbiol. 26* (3), 229−242.
(6) Banas, J. A., and Drake, D. R. (2018) Are the mutans streptococci still considered relevant to understanding the microbial etiology of dental caries? *BMC Oral Health 18* (1), 129.
(7) Donia, M. S., Cimermancic, P., Schulze, C. J., Wieland Brown, L. C., Martin, J., Mitreva, M., Clardy, J., Linington, R. G., and Fischbach, M. A. (2014) A systematic analysis of biosynthetic gene clusters in the human microbiome reveals a common family of antibiotics. *Cell 158* (6), 1402−1414.
(8) Donia, M. S., and Fischbach, M. A. (2015) HUMAN MICROBIOTA. Small molecules from the human microbiota. *Science 349* (6246), 1254766.
(9) Merritt, J., and Qi, F. (2012) The mutacins of Streptococcus mutans: regulation and ecology. *Mol. Oral Microbiol. 27* (2), 57−69.
(10) Joyner, P. M., Liu, J., Zhang, Z., Merritt, J., Qi, F., and Cichewicz, R. H. (2010) Mutanobactin A from the human oral pathogen *Streptococcus mutans* is a cross-kingdom regulator of the yeast-mycelium transition. *Org. Biomol. Chem. 8* (24), 5486−9.
(11) Liu, L., Hao, T., Xie, Z., Horsman, G. P., and Chen, Y. (2016) Genome mining unveils widespread natural product biosynthetic capacity in human oral microbe *Streptococcus mutans*. *Sci. Rep. 6*, 37479.
(12) Hao, T., Xie, Z., Wang, M., Liu, L., Zhang, Y., Wang, W., Zhang, Z., Zhao, X., Li, P., Guo, Z., Gao, S., Lou, C., Zhang, G., Merritt, J., Horsman, G. P., and Chen, Y. (2019) An anaerobic bacterium host system for heterologous expression of natural product biosynthetic gene clusters. *Nat. Commun. 10* (1), 3665.
(13) Lin, X. B., Lohans, C. T., Duar, R., Zheng, J., Vederas, J. C., Walter, J., and Ganzle, M. (2015) Genetic determinants of reutericyclin biosynthesis in *Lactobacillus reuteri*. *Appl. Environ. Microbiol. 81* (6), 2032−41.
(14) Holtzel, A., Ganzle, M. G., Nicholson, G. J., Hammes, W. P., and Jung, G. (2000) The first low molecular weight antibiotic from lactic acid bacteria: reutericyclin, a new tetramic acid. *Angew. Chem., Int. Ed. 39* (15), 2766−2768.
(15) Ganzle, M. G. (2004) Reutericyclin: biological activity, mode of action, and potential applications. *Appl. Microbiol. Biotechnol. 64* (3), 326−32.
(16) Argimon, S., Konganti, K., Chen, H., Alekseyenko, A. V., Brown, S., and Caufield, P. W. (2014) Comparative genomics of oral isolates of *Streptococcus mutans* by *in silico* genome subtraction does not reveal accessory DNA associated with severe early childhood caries. *Infect., Genet. Evol. 21*, 269−78.
(17) Böhme, R., Jung, G., and Breitmaier, E. (2005) Synthesis of the antibiotic (*R*)-reutericyclin via dieckmann condensation. *Helv. Chim. Acta 88* (11), 2837−2841.
(18) Clemens, R. J., and Hyatt, J. A. (1985) Acetoacetylation with 2,2,6-trimethyl-4H-1,3-dioxin-4-one: a convenient alternative to diketene. *J. Org. Chem. 50* (14), 2431−2435.
(19) Gaudelli, N. M., and Townsend, C. A. (2014) Epimerization and substrate gating by a TE domain in beta-lactam antibiotic biosynthesis. *Nat. Chem. Biol. 10* (4), 251−8.
(20) Hayashi, A., Saitou, H., Mori, T., Matano, I., Sugisaki, H., and Maruyama, K. (2012) Molecular and catalytic properties of monoacetylphloroglucinol acetyltransferase from *Pseudomonas* sp. YGJ3. *Biosci., Biotechnol., Biochem. 76* (3), 559−66.
(21) Pavkov-Keller, T., Schmidt, N. G., Zadlo-Dobrowolska, A., Kroutil, W., and Gruber, K. (2019) Structure and Catalytic Mechanism of a Bacterial Friedel-Crafts Acylase. *ChemBioChem 20* (1), 88−95.
(22) Vilchez, R., Lemme, A., Ballhausen, B., Thiel, V., Schulz, S., Jansen, R., Sztajer, H., and Wagner-Dobler, I. (2010) *Streptococcus mutans* inhibits *Candida albicans* hyphal formation by the fatty acid signaling molecule trans-2-decenoic acid (SDSF). *ChemBioChem 11* (11), 1552−62.
(23) Cherian, P. T., Wu, X., Maddox, M. M., Singh, A. P., Lee, R. E., and Hurdle, J. G. (2015) Chemical modulation of the biological activity of reutericyclin: a membrane-active antibiotic from *Lactobacillus reuteri*. *Sci. Rep. 4*, 4721.
(24) Lamont, R. J., Koo, H., and Hajishengallis, G. (2018) The oral microbiota: dynamic communities and host interactions. *Nat. Rev. Microbiol. 16* (12), 745−759.

(25) Kreth, J., Giacaman, R. A., Raghavan, R., and Merritt, J. (2017) The road less traveled - defining molecular commensalism with *Streptococcus sanguinis*. *Mol. Oral Microbiol. 32* (3), 181−196.
(26) Aleti, G., Baker, J. L., Tang, X., Alvarez, R., Dinis, M., Tran, N. C., Melnik, A. V., Zhong, C., Ernst, M., Dorrestein, P. C., and Edlund, A. (2019) Identification of the Bacterial Biosynthetic Gene Clusters of the Oral Microbiome Illuminates the Unexplored Social Language of Bacteria during Health and Disease. *mBio 10* (2), e00321−19.
(27) Li, Y., Li, Z., Yamanaka, K., Xu, Y., Zhang, W., Vlamakis, H., Kolter, R., Moore, B. S., and Qian, P. Y. (2015) Directed natural product biosynthesis gene cluster capture and expression in the model bacterium *Bacillus subtilis*. *Sci. Rep. 5*, 9383.
(28) Perry, D., and Kuramitsu, H. K. (1981) Genetic transformation of Streptococcus mutans. *Infect. Immun. 32* (3), 1295−7.
(29) Baker, J. L., Lindsay, E. L., Faustoferri, R. C., To, T. T., Hendrickson, E. L., He, X., Shi, W., McLean, J. S., and Quivey, R. G. (2018) Characterization of the Trehalose Utilization Operon in *Streptococcus mutans* Reveals that the TreR Transcriptional Regulator Is Involved in Stress Response Pathways and Toxin Production. *J. Bacteriol. 200* (12), e00057-18.

NOTE ADDED AFTER ASAP PUBLICATION

This paper was published on the Web on January 10, 2020. Additional statistical significance in the caption for Figure 3 was added, and the corrected version was reposted on January 14, 2020.

https://dx.doi.org/10.1021/acsinfecdis.9b00365
ACS Infect. Dis. 2020, 6, 563−571